Send Orders for Reprints to reprints@benthamscience.ae

566 *Current Alzheimer Research,* 2016, *13,* 566-574

Hippocampal Subfield Atrophies in Converted and Not-Converted Mild Cognitive Impairments Patients by a Markov Random Fields Algorithm

Roberta Vasta[a,§], Antonio Augimeri[a,§], Antonio Cerasa[a,*] , Salvatore Nigro[a] , Vera Gramigna[c], Matteo Nonnis[a], Federico Rocca[a], Giancarlo Zito[d], Aldo Quattrone[a,b] for the Alzheimer's Disease Neuroimaging Initiative[#]

[a]*Neuroimaging Unit, Institute of Bioimaging and Molecular Physiology-CNR, Germaneto (CZ), Italy;* [b]*Institute of Neurology , University "Magna Graecia", Germaneto (CZ), Italy;* [c]*Università degli Studi "Magna Graecia", Dipartimento di Scienze Mediche e Chirurgiche, Germaneto (CZ), Italy;* [d]*Laboratory of Electrophysiology for Translational neuroScience (LET'S), ISTC, National Research Council at 'S. Giovanni Calibita' Fatebenefratelli Hospital, Rome, Italy*

Antonio Cerasa

Abstract: Although measurement of total hippocampal volume is considered as an important hallmark of Alzheimer's disease (AD), recent evidence demonstrated that atrophies of hippocampal subregions might be more sensitive in predicting this neurodegenerative disease. The vast majority of neuroimaging papers investigating this topic are focused on the difference between AD and patients with mild cognitive impairment (MCI), not considering the impact of MCI patients who will or not convert in AD. For this reason, the aim of this study was to determine if measurements of hippocampal subfields provide advantages over total hippocampal volume for discriminating these groups. Hippocampal subfields volumetry was extracted in 55 AD, 32 converted and 89 not-converted MCI (c/nc-MCI) and 47 healthy controls, using an atlas-based automatic algorithm based on Markov random fields embedded in the Freesurfer framework. To evaluate the impact of hippocampal atrophy in discriminating the insurgence of AD-like phenotypes we used three classification methods: Support Vector Machine, Naïve Bayesian Classifier and Neural Networks Classifier. Taking into account only the total hippocampal volume, all classification models, reached a sensitivity of about 66% in discriminating between c-MCI and nc-MCI. Otherwise, classification analysis considering all segmenting subfields increased accuracy to diagnose c-MCI from 68% to 72%. This effect resulted to be strongly dependent upon atrophies of the subiculum and presubiculum. Our multivariate analysis revealed that the magnitude of the difference considering hippocampal subfield volumetry, as segmented by the considered atlas-based automatic algorithm, offers an advantage over hippocampal volume in distinguishing early AD from nc-MCI.

Keywords: Atrophy, automated segmentation, classification models, freesurfer, hippocampal subfields, mild cognitive impairment, volumetry.

1. INTRODUCTION

The most common cause of neurodegenerative dementia in the elderly population is Alzheimer's disease (AD). The clinical diagnosis of AD requires the presence of multiple cognitive deficits, including memory impairment, whereas the underlying pathological processes appear to begin and covertly progress several years before. As a consequence, an increased interest has been focused on identifying mild cognitive deficits characteristic of the preclinical phase of AD in order to slow down or prevent disease progression.

Mild cognitive impairment (MCI) is a transitional phase characterized by memory disturbance in the absence of dementia, followed by widespread cognitive deficits in multiple domains until a disability threshold is reached and traditional diagnostic criteria for probable AD are fulfilled [1, 2]. In particular, studies have shown that MCI patients convert to AD at an annual rate of 10–15% per year [3]. It is known that MCI patients who do not convert to AD either remain stable or develop other forms of dementia or, very rarely, revert to normal status [4].

In the past 20 years, a considerable effort has been put into the development of advanced neuroimaging processing techniques in order to identify biomarkers that could reliably improve the diagnostic confidence of clinical diagnosis. In particular, the importance of imaging in AD diagnosis has been underlined by the inclusion of imaging markers in new criteria proposed for earlier diagnosis of AD [1, 5]. For several years, it has been proposed that among all the MRI markers of AD [6], hippocampal atrophy assessed on high-resolution T1-weighted MRI is one of the most significant and consistent markers of progression of AD [1].

*Address correspondence to this author at the IBFM-CNR, Viale Europa, 88100 Germaneto (CZ), Italy; Tel: +39-0961-3695904; Fax: +39-0961-3695919; E-mail: a.cerasa@unicz.it

[#]*Data used in preparation of this article were obtained from the Alzheimer's Disease Neuroimaging Initiative (ADNI) database (adni.loni.usc.edu). As such, the investigators within the ADNI contributed to the design and implementation of ADNI and/or provided data but did not participate in analysis or writing of this report. A complete listing of ADNI investigators can be found at: at: http://adni.loni.usc.edu/wp-content/uploads/how_to_apply/ADNI_Acknowledgement_List.pdf.*

[§]*These authors equally contributed to this work*

1875-5828/16 $58.00+.00

However, in the last few years, several lines of evidence proposed that the measure of the total hippocampal volume might not be sufficiently sensitive to discriminate AD-like phenotypes. This hypothesis is based upon the fact that approximately 30% of patients in pre-clinical stage of AD (MCI), which will convert to AD in the next 18 months, do not have prominent hippocampal atrophy at basal MRI [7].

Moreover, the volumetric evaluation of a whole structure cannot provide information about the contribution of specific subregions in atrophy or expansion, thus preventing a properly detailed disease-related regional impairment. Indeed, hippocampus is not a homogenous structure, consisting of several histologically distinct subfields: subiculum, cornu ammonis sectors (CA1-3) and dentate nucleus [8]. The existence of different pathways (meaning different memory processing) and distinctive histological characteristics suggests that hippocampal subfields might be involved in the course of AD-related neurodegeneration at different stages. Several post-mortem studies [9-10] have indeed demonstrated that tau pathology, neuronal loss and tangles accumulation first affect the transentorihnal region of the perinhinal cortex, followed by the entorhinal cortex and the CA1 subfield, finally extending into the CA4 and the subiculum, which stresses the importance of the choice of boundary selection during the segmentation [11].

Preliminary neuroimaging studies confirmed this regional predominance of AD-related pathological changes, demonstrating that volumetric losses of the CA1 and subiculum are more sensitive than total hippocampus volume to the effects of AD pathology burden [12-19]. However, at least two confounding variables limit the sensitivity of hippocampal volume as biomarker of AD: first, the vast majority of these studies performed univariate analysis contrasting AD patients with respect to MCI; second, there is considerable heterogeneity among MCI patients: some remain stable for a long time, others revert to normal cognitive status, and still others develop dementia other than AD [20]. For this reason, the definition of reliable neuroimaging markers useful to identify an MCI patient at risk of developing AD has not been completely achieved yet.

The purpose of this study was to determine if measurements of hippocampal subfields provide advantages over the total hippocampal volume for discriminating the two critical early phases of AD: MCI who will or will not convert to AD. To do that, we employed a new computational method coming from Fischl's group (Martinos Center for Biomedical Imaging, Boston, Massachusetts; http://surfer.nmr.mgh. harvard.edu/). This method allows fully automated segmentation of the hippocampus subfields from conventional structural images, by Bayesian techniques using Markov random field shape priors learned from manual segmentations. The accuracy of this method evaluated against manual segmentations has already been demonstrated [21].

To evaluate the diagnostic accuracy of global hippocampal atrophy against the hippocampal subfield volumetry in discriminating between the two subtypes of MCI we employed three different multivariate classification methods: Support Vector Machine (SVM), Naïve Bayesian Classifier (NBC) and Neural Networks Classifier (NNC). In order to be consistent with previous neuroimaging studies and to increase the statistical robustness of our investigation, we used data from the Alzheimer's disease Neuroimaging Initiative database (adni.loni.usc.edu).

2. MATERIALS AND METHOD

2.1. Data

Data used in the preparation of this article were obtained from the Alzheimer's disease Neuroimaging Initiative (ADNI) database (adni.loni.usc.edu). The ADNI was launched in 2003 by the National Institute on Aging (NIA), the National Institute of Biomedical Imaging and Bioengineering (NIBIB), the Food and Drug Administration (FDA), private pharmaceutical companies and non-profit organizations, as a $60 million, 5-year public-private partnership. The primary goal of ADNI has been to test whether serial magnetic resonance imaging (MRI), positron emission tomography (PET), other biological markers, and clinical and neuropsychological assessment can be combined to measure the progression of mild cognitive impairment (MCI) and early Alzheimer's disease (AD). Determination of sensitive and specific markers of very early AD progression is intended to aid researchers and clinicians to develop new treatments and monitor their effectiveness, as well as lessen the time and cost of clinical trials.

We considered all the subjects for whom preprocessed images were available. We selected 223 patients from the Alzheimer's disease Neuroimaging Initiative (ADNI) repository (adni.loni.usc.edu): 47 cognitively normal elderly controls (CTR), 55 patients with AD, 32 patients with MCI who had converted to AD within 18 months (c-MCI) and 89 patients with a MCI stable status (nc-MCI). We did not consider MCI patients who had been followed up for less than 18 months without converting within this time frame. Demographical data of this group are shown in Table **1**. The identification numbers of the images used in this study are reported in Table **S1** of supplementary materials.

2.2. MRI Acquisition

Images were all T1 weighted structural MRI scans from 1.5 T scanners acquired using a 3D MPRAGE sequence. MRI acquisition had been done according to the ADNI acquisition protocol in [22]. For each subject, we used the MRI scan from the baseline visit when available and from the screening visit otherwise. To enhance standardization across sites and platforms of images acquired in the ADNI study, pre-processed images that have undergone some post-acquisition correction of certain image artifacts are available [22]. We used those corrected in image geometry for gradient nonlinearity and corrected for intensity non-uniformity due to non-uniform receiver coil sensitivity. All subjects were scanned twice at each visit. As explained in [22], MR scans were graded qualitatively by the ADNI investigators of the ADNI MRI quality control center at the Mayo Clinic for artifacts and general image quality. Each scan was graded on several separate criteria: blurring/ghosting, flow artifact, intensity and homogeneity, signal-to-noise ratio (SNR), susceptibility artifacts, and gray-white/cerebrospinal fluid contrast. For each subject, we used the MRI scan which was considered as the "best" quality scan by the ADNI investiga-

Table 1. Clinical characteristics of subjects.

	CTR	ncMCI	cMCI	AD	F/p level (ANOVA)	Post-hoc t-test (cMCI vs ncMCI)
N°	47	89	32	55		
Age	78.19±4.4	75.42	75.53	75.89±6	F=2.04/	p=0.938
	0	±7.18	±7.38	.35	p=0.109	
Gender	31; 65.96	58;	22;	35;	p=0.970	p=0.714
(*n*°; % male)		65.17	59.46	63.64		
MMSE	28.96±1.1	27.20	26.81	19.11±5	F=68.68/	p=0.290
	4	±1.71	±1.96	.73	p<0.0001	
Global CDR	0.09±0.22	0.50±	0.50±	1.09±0.	F=103.07/	p=0.999
		0.00	0.00	69	p<0.0001	
GDSCALE	1.19±1.61	1.72±	1.53±	1.85±1.	F=1.75/	p=0.548
		1.51	1.50	61	p=0.16	

Key: CTR. healthy elderly people; nc-MCI. stable mild cognitive impairment; c-MCI. converted mild cognitive impairment; AD. Alzheimer's.

tors (see Supplementary Materials). In the description of the ADNI methods (adni.loni.usc.edu), the "best" quality image is the one that was used for the complete pre-processing steps. We thus used the images which had been selected for the complete preprocessing pipeline. No other exclusion criteria based on image quality were applied.

2.3. Data Analysis

2.3.1. Hippocampal Subfield Segmentation-Freesurfer

The hippocampal segmentation was carried out by using two successive steps. The whole hippocampus was initially segmented by completing the FreeSurfer image analysis pipeline (Martinos Center for Biomedical Imaging, Boston, Massachusetts), that is documented and freely available for download online (http://surfer.nmr.mgh.harvard.edu/). The technical details of these procedures were described in previous publications [23-26].

In brief, the processing steps relevant to this work include removal of nonbrain tissue by using a hybrid watershed/surface deformation procedure [25], automated Talairach transformation, and segmentation of the subcortical white matter and deep gray matter volumetric structures (including hippocampus, amygdala, caudate, putamen, and ventricles) [26]. Visual inspection and quality control of hippocampal segmentations was carried out for all subjects. The estimated intracranial volume (ICV) was also calculated.

Next, automated segmentation of the hippocampus to its respective subfields was performed by using Bayesian inference and a statistical model of the medial temporal lobe. In particular, a probabilistic atlas mesh has been previously built from the manual delineation of the hippocampus of control subjects [21]. A tetrahedrical mesh covering the image domain of interest is defined, which is deformed from its reference position by sampling from a Markov random field model regulating the position of the mesh nodes. The probabilistic atlas is defined by the connectivity of its tetrahedral mesh and the probabilities of label occurrences.

Freesurfer provides an automatic segmentation of hippocampus in seven subfields: CA1, CA2–3, CA4-DG, subiculum, presubiculum, fimbria, and hippocampal fissure. It was shown that the Dice overlap measures between manual and automated segmentation methods were approximately 0.7 for all the substructures (from CA2–3 and subiculum at 0.74 to CA1 at 0.62). For more details about this technique, and particularly about the borders used to define the different subfields, see Van Leemput *et al.* 2009 [21]. Fig. (**1**) shows an example of subfield segmentation obtained by the automatic algorithm based on Markov random fields embedded in the Freesurfer framework.

2.3.2. Univariate Analysis

Univariate analysis was carried out using MATLAB (Matlab version R2012b, The MathWorks, Natick, MA). First, to assess differences in demographical data among groups we used ANOVA analysis for age and clinical data and Pearson's chi-square test for gender.

Next, for each hemisphere we performed a one-way ANCOVA analysis to investigate differences among the four groups in both the global hippocampal volume and hippocampal subfield volumes. Age and gender were included in the model as covariates of no interest. Post-hoc analysis (Tukey *t*-tests) were performed to investigate differences between MCI subtypes.

To take into account the inter-individual variability, all the volumes were normalized by ICV value, where $volume_{norm}=(volume_{raw}/ICV)*1{,}000$. Significance level was set at 0.01 (number of comparisons (4) / 0.05= 0.012).

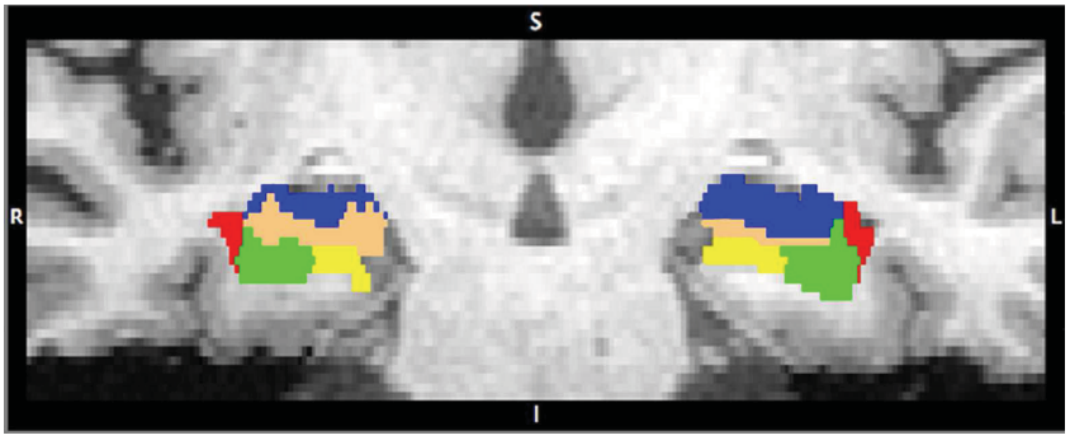

Fig. (1). Hippocampal subfields segmentation.

2.3.3. Multivariate Analysis

In the classification analysis, we compared performances of the whole normalized hippocampal volume and the set of all normalized subfield volumes. Since we want to evaluate whether hippocampal subfield volumes can be used to improve the AD diagnostic accuracy from the preclinical phase to clinical dementia, thus discriminating between c-MCI and nc-MCI patients, we selected three different classification methods: Support Vector Machine (SVM), Naïve Bayesian Classifier (NBC) and Neural Networks Classifier (NNC). All these algorithms were embedded in the MATLAB Statistics Toolbox.

In each model, we first used the set of features relative to AD and CTR as training sample and then tested the obtained model to classify the MCI population in c-MCI and nc-MCI. The assumption behind this hypothesis is that the subpopulation of c-MCI may represent an imaging profile more similar to AD subjects than nc-MCI [4].

The SVM model was based on the LIBSVM tool [27], which provides different SVM formulations, several kernel functions and many cross validation strategies. Among several tuning option provided by the tool we set a linear kernel function. Since the training data is not linearly separable, we used a Soft Margin SVM formulation. Using LIBSVM, such a model can be built by specifying the C parameter. This parameter controls the tradeoff between a wide margin and the number of instances not meeting the margin criteria. Small C values allow a large margin of separation, but also permit a lot of misclassificated instances on the training data. Taking a large C, it increases the number of instances that meet the margin criteria, but cause a small margin of separation. To select a proper value for C, we used the built-in validation method of LIBSVM that tests for different parameter values in orders of magnitude and selects the one with the best performance. The C values for the different SVM models are reported below: 1 (default) for E1 and 0.01 for E2. Since we tested the models on the dataset formed by c-MCI and nc-MCI that was not employed in the training phase, no cross validation strategy was used.

The NBC was implemented using MATLAB: to estimate the model, a normal distribution was chosen to model each predictor. To estimate the prior probability we used the class relative frequencies distribution. The fitted parameters of the normal distributions (mean and standard deviation) used in classifiers are reported in Table **S2** of supplementary materials for each class and attributes.

The NNC was implemented using the Neural Network Pattern Recognition Tool integrated in MATLAB: we adopted quite common setting in pattern recognition. Our schema consisted of two-layer feedforward network, with sigmoid transfer function in both hidden and output layer. We trained the network using a batch mode procedure based upon the so-called Resilient Backpropagation Algorithm. This method converges generally much faster than other descendent methods and it is an adequate choice when NNs are employed in pattern recognition problem [28]. The number of input neurons was 2 in the experiment E1 and 7 in E2 to match the number of input volumes in each experiment. To determinate the best number of hidden units, an optimization procedure was carried out for each model. Since this number depends in a complex way on many factors (the number of training cases, the amount of noise or the complexity of the classification to be learned), the performance of each model were evaluated varying the number of units in the hidden layer in a range from 2 to 20. The best configuration was 7 hidden nodes for E1 and 14 hidden nodes for E2.

Each model was evaluated in two different settings. In the first experiment (E1) the total hippocampal volume for both sides was used. In a second experiment (E2), models were built upon the set of hippocampal subfield volumes (CA1, CA2–3, CA4-DG, subiculum, presubiculum, fimbria, and hippocampal fissure) for each hemisphere. Moreover, in order to investigate the presence of subfields more informative of MCI conversion, receiving operating characteristic (ROC) curves were calculated for each subfield volume, using Perfcurve function of MATLAB Statistics Toolbox. Roc curves provide a graphical representation of the model's goodness in discriminating among groups by a plot of the true positive rate (sensitivity) versus the false positive rate (1-specificity) for various thresholds. The discriminatory power was expressed by the area under the curve (AUC). AUC statistical comparisons among subfields in distinguish between nc-MCI and c-MCI were carried out to establish whether more informative subfields exist.

3. RESULTS

3.1. Univariate Analysis

There was no significant difference in demographic and depression scales between all groups as shown in the Table **1**, whereas, obviously, AD patients showed the lowest scores in cognitive tests (MMSE and global CDR). Of note, post-hoc analysis (Tukey *t*-tests) revealed not significant differences in all demographic and clinical variables between the two MCI subtypes.

Table **2** showed differences among all groups in total hippocampal volumes and hippocampal subfield volumes, both of them normalized by ICV. Overall, ANCOVA analysis revealed well-known patterns of hippocampal atrophy including either the total hippocampus or subfields (in particular the subiculum, presubiculum, CA1-4 and Fimbria) in AD patients. Post-hoc analysis (Tukey *t*-tests) comparing the two MCI subtypes, revealed that the total right Hippocampal volume allows to differentiate patients who will converted from those who will not. A similar significant volume reduction in c-MCI compared to nc-MCI was also observed when considering subiculum, presubiculum and CA4-DG.

3.2. Multivariate Analysis

Given the intrinsic limitation of univariate analysis in discriminating groups at the group level only, next we performed multivariate analysis with the aim to define new reliable biomarkers of early AD.

First, we applied classification models to determine the Accuracy, Sensitivity and Specificity using left and right hippocampal volumes as features in the training set (Table **3**). All models reached similar, sufficient, performance in the individual classification of patients with nc-MCI and c-MCI, with an accuracy value of about 66%.

Next, the result reported in Table **4** were referred to the model trained using the whole set of subfield volumes. All classifiers performed better than in the previous case and the best result is achieved by the NN model, reaching 72% of accuracy.

Lastly, the AUC statistical comparisons among subfields suggested that subiculum and presubiculum are more informative than the other hippocampal subregions in discriminating between nc-MCI and c-MCI, with AUC values of 0.76 and 0.77 respectively (see Table **5**). ROC curves for each subfield volume are displayed in Fig. (**2**).

4. DISCUSSION

Growing interest has developed in hippocampal subfield volumetry over the past few years in order to use this anatomical metric as biomarkers for the early diagnosis of Alz-

Table 2. **ANCOVA analysis. Normalized hippocampal total volumes and subfields volumes (mean ± standard deviation) in all groups are showed. Post-hoc t-test (Tukey) has been reported for the comparison between MCI subtypes.**

Anatomic al Features	CTR	MCIc	MCs	AD	F/p-level	Post-hoc t-test (cMCI vs ncMCI)
Right Hipp	36.27 ±4.46	28.94 ±5.95	32.61 ±5.10	25.88 ±5.47	F= 26.9 / P< 0.000001	P=0.0003
Left Hipp	34.29 ±5.45	28.11 ±5.54	32.08 ±5.95	25.86 ±5.16	F= 19.8 / P< 0.000001	P=0.06
Right PreSub	2.57± 0.34	2.11± 0.93	2.45± 0.37	1.97± 0.32	F= 44.1 / P< 0.000001	P=0.00009
Left PreSub	2.59± 0.44	2.12± 0.33	2.48± 0.46	2.01± 0.34	F= 28.1 / P< 0.000001	P=0.001
Right CA1	2.20± 0.28	1.92± 0.29	2.01± 0.24	1.82± 0.29	F= 20.2 / P< 0.000001	P=0.56
Left CA1	2.06± 0.35	1.89± 0.30	1.97± 0.27	1.89± 0.29	F= 4.1/ P=0.007	P=0.65
Right CA 23	6.03± 0.74	5.41± 0.92	5.94± 0.78	5.10± 0.75	F= 19.7 / P< 0.000001	P=0.02
Left CA 23	5.52± 1.00	5.02± 0.73	5.58± 0.88	4.92± 0.64	F= 10.6 / P=0.0000 02	P=0.03
Right Fimbria	0.27± 0.10	0.19± 0.14	0.22± 0.12	0.16± 0.11	F= 10.7 / P=0.000001	P=0.67
Left Fimbria	0.29± 0.13	0.21± 0.12	0.26± 0.15	0.16± 0.13	F= 10.5 / P=0.000002	P=0.51
Right Sub	3.74± 0.43	3.03± 0.52	3.55± 0.54	2.81± 0.43	F= 49.8 / P< 0.000001	P=0.00005
Left Sub	3.60± 0.57	3.04± 0.55	3.57± 0.61	2.86± 0.45	F= 29.5 / P= 0.000002	P=0.0003
Right CA4DG	3.36± 0.42	2.91± 0.50	3.25± 0.45	2.71± 0.41	F= 28.8 / P< 0.000001	P=0.008
Left CA4DG	3.13± 0.54	2.68± 0.44	3.05± 0.53	2.59± 0.39	F= 18.5 / P< 0.000001	P=0.009
Right Fissure	0.31± 0.16	0.24± 0.12	0.30± 0.17	0.24± 0.15	F= 3.1 / P= 0.02	P=0.38
Left Fissure	0.26± 0.16	0.23± 0.11	0.27± 0.14	0.24± 0.17	F= 0.77 / P=0.55	P=0.71

Key: CTR. healthy elderly people; nc-MCI. stable mild cognitive impairment; c-MCI. converted mild cognitive impairment; AD. Alzheimer's disease; CDR. Clinical Dementia Rating; MMSE. Mini Mental State Examination; GDS. Geriatric Depression Scale.

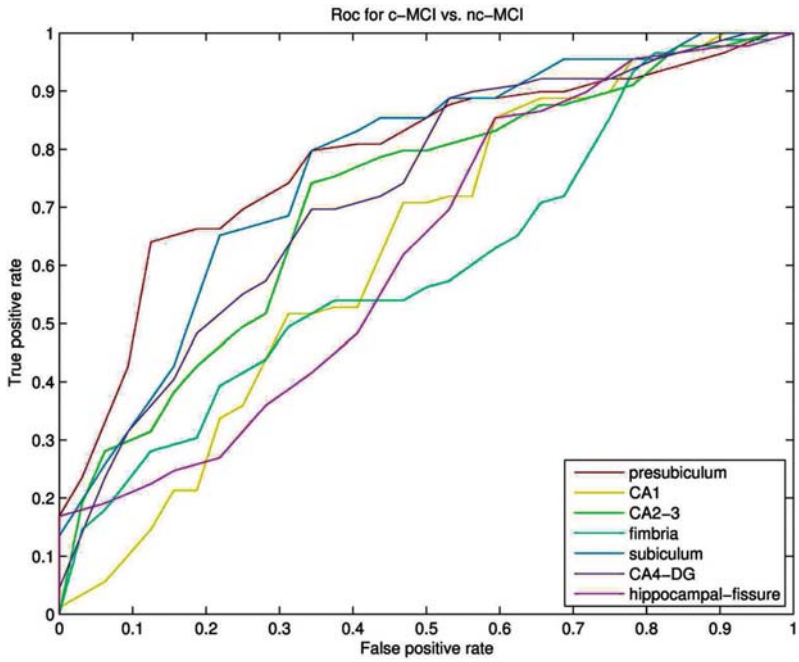

Fig. (2). Receiving operating characteristic (ROC) curves comparison among hippocampal subfield volumes in the individual discrimination between c-MCI and nc-MCI.

heimer's disease. Aim of this study was to determine if measurements of hippocampal subfields provide advantages over total hippocampal volume for discriminating MCI individuals who are (or not) suffering from prodromal AD. Advanced automatic hippocampal measurements were obtained by applying a new validated algorithm based on Markov random fields embedded in the Freesurfer framework.

Table 3. Classification performances of whole Hippocampal Volume in the individual discrimination between c-MCI and nc-MCI.

Mode	Accuracy	Sensitivity	Specificity
SVM	0.6612	0.6404	0.7188
NN	0.6694	0.6517	0.7188
NB	0.6529	0.6292	0.7188

SVM: Support Vector Machine; NBC: Naïve Bayesian Classifier; NNC: Neural Networks Classifier.

Table 4. Classification performances of Hippocampal Subfield Volumes in the individual discrimination between c-MCI and nc-MCI.

Mode	Accuracy	Sensitivity	Specificity
SVM	0.7107	0.6966	0.7500
NN	0.7273	0.6966	0.8125
NB	0.6860	0.6742	0.7188

SVM: Support Vector Machine; NBC: Naïve Bayesian Classifier; NNC: Neural Networks Classifier.

Table 5. Area under curve (AUC) comparison among subfield volumes in the individual discrimination between c-MCI and nc-MCI.

Anatomical features	AUC (Area Under Curve)
CA1	0.6166
CA23	0.7012
CA4DG	0.7128
Fimbra	0.5864
Sub	0.7573
PreSub	0.7746
Hipp Fissure	0.6096

Historically MRI-based hippocampal volume measurement has been proposed as potential biomarker for the early AD diagnosis [1]. However the accuracy of this measurement may be limited by a moderate sensitivity and a rather low specificity to AD pathophysiological processes. This later hypothesis has been recently proved by a large amount of post-mortem [9, 10, 29-31] and neuroimaging studies [15-17, 19, 32-36] which demonstrated that neurofibrillary pathology and neuronal loss differentially harm hippocampal subregions early in the AD course. The first neuroimaging evidence on the presence of regional hippocampal abnormalities in AD patients derived from manual delineation [16, 17], describing the presence of a specific involvement of the subiculum and CA sectors. However, this kind of method is time-consuming and dependent on rater experience, thus making it difficult to assess reliability between the methods

and the application on large samples. With the advent of advanced neuroimaging algorithms, new methods performing fully automated measurements and segmentation of microstructural changes in the hippocampal subregions have been proposed [37-40]. Although, these studies confirmed the selective patterns of atrophies in hippocampal subfields described in post-mortem studies, they generally reported differences between patients and controls only at a group level, thus with a very limited translation to an individual diagnosis in more clinical settings.

Another limitation, in this field of study, is the less attention paid to the use of hippocampal subfields as markers to classify MCI patients who remained stable (nc-MCI) and MCI who deteriorated to AD (c-MCI). Up to now, there are very few studies in this specific topic. For instance, in a longitudinal study, Frankò *et al.* [39] comparing the hippocampal atrophy rates maps of progressive MCI patients and stable MCI, described higher atrophy rates in the antero-lateral region of the right hippocampus for the first group. They also showed that the atrophy rate of this region is able to discriminating between these two groups with a sensitivity value of 74.4 %.

In line with this latter evidence, we demonstrated that, using three different classification models for classifying MCI patients who convert in AD from MCI patients who remain stable, combined subfield volumes overcome the accuracy obtained when total hippocampal volume was entered in the model (72% versus 66%). The obtained accuracy improvement confirmed the hypothesis that microstructural changes in the hippocampal subregions may have a higher specificity, thus reinforcing a better identification of MCI-related neurodegenerative processes.

Our work is one of the first multivariate neuroimaging study which addresses the potential of hippocampal subfield volumetry in improving the diagnostic accuracy for discriminating between MCI individuals who are or not suffering from prodromal AD. Among all hippocampal subfields, subiculum and presubiculum demonstrated the greatest discriminant power in distinguish nc-MCI from c-MCI. This pattern of hippocampal subfield loss is in agreement with previous post-mortem and neuroimaging studies [14, 38, 40, 41] and highlighted the role of the subicular region in AD-related neurodegenerative processes. Indeed, the subiculum provides the principal neocortical output of the hippocampus through fibers that are part of the alveus and the fimbria [8]. Therefore, subicular atrophy could be interpreted as the consequence of neurodegeneration and metabolic derangement of the CA1 subfield [11] or as a structural modification occurring in response to an altered network connectivity.

However, automated hippocampal subfield segmentation as performed by Freesurfer is not without limitations. As recently reviewed by Wisse *et al.* [42], Freesurfer algorithms are characterized by some concerns. For instance, the parcelation scheme used by FreeSurfer for the segmentation is based on the subfield distribution in one coronal section in the body of the hippocampus [42]. This means that subfields were segmented along the complete long axis of the hippocampus. However, the presence and position of the subfields differ along this axis [8, 42]. Consequently, the locations of the boundaries between subfields in this segmentation protocol might be in mismatch with the anatomical atlases in a large part of the long axis.

CONCLUSION

In conclusion, using three different classification models, we concluded that hippocampal subfield measurement provides a more classification accuracy, compared to global hippocampal volume, in discriminating MCI individuals who are suffering from prodromal AD. Although the obtained performance are in line with literature, these improvements are not enough to demonstrate that hippocampal subfields, as segmented by Freesurfer, might be considered as a reliable biomarker with a high translational potential in everyday clinical practice. Given the constant technical advances, it is likely that some of the limitations inherent to Freesurfer algorithms will be overcome in the next years. However, considering the performance reached by other groups using different hippocampal subfield segmentation approaches [37-40], we retain that a useful future improvement will derive from the implementation of a multimodal approach. Indeed, while anatomical MRI is the main structural neuroimaging method used in most AD studies and clinical trials, diffusion tensor images (DTI) is sensitive to microscopic white matter (WM) changes not detectable with standard MRI, offering additional markers of neurodegeneration. A large amount of evidence has recently raises doubts about the sensitivity of hippocampal volume measurements [43] to detect brain alterations that could be the earliest signs of AD. In fact, it is well-known that DTI metric detected in the hippocampus is a better neuroradiologic marker of underlying memory decline than volume [44]. For this reason, the use of combined biomarkers seems to be a rational and a future promising approach for enhancing diagnostic accuracy in identifying AD-like phenotypes.

SUPPLEMENTARY MATERIAL

Supplementary material is available on the publisher's web site along with the published article.

CONFLICT OF INTEREST

The authors confirm that this article content has no conflict of interest.

ACKNOWLEDGEMENTS

Data collection and sharing for this project was funded by the Alzheimer's Disease Neuroimaging Initiative (ADNI) (National Institutes of Health Grant U01 AG024904) and DOD ADNI (Department of Defense award number W81XWH-12-2-0012). ADNI is funded by the National Institute on Aging, the National Institute of Biomedical Imaging and Bioengineering, and through generous contributions from the following: Alzheimer's Association; Alzheimer's Drug Discovery Foundation; Araclon Biotech; BioClinica, Inc.; Biogen Idec Inc.; Bristol-Myers Squibb Company; Eisai Inc.; Elan Pharmaceuticals, Inc.; Eli Lilly and Company; EuroImmun; F. Hoffmann-La Roche Ltd and its affiliated company Genentech, Inc.; Fujirebio; GE Healthcare; IXICO Ltd.; Janssen Alzheimer Immunotherapy Research & Development, LLC.; Johnson & Johnson Pharmaceutical Research

& Development LLC.; Medpace, Inc.; Merck & Co., Inc.; Meso Scale Diagnostics, LLC.; NeuroRx Research; Neurotrack Technologies; Novartis Pharmaceuticals Corporation; Pfizer Inc.; Piramal Imaging; Servier; Synarc Inc.; and Takeda Pharmaceutical Company. The Canadian Institutes of Health Research is providing funds to support ADNI clinical sites in Canada. Private sector contributions are facilitated by the Foundation for the National Institutes of Health (www.fnih.org). The grantee organization is the Northern California Institute for Research and Education, and the study is coordinated by the Alzheimer's Disease Cooperative Study at the University of California, San Diego. ADNI data are disseminated by the Laboratory for Neuro Imaging at the University of Southern California.

REFERENCES

[1] Frisoni GB, Fox NC, Jack CR Jr, Scheltens P, Thompson PM. The clinical use of structural MRI in Alzheimer disease. Nat Rev Neurol 6(2): 67-77 (2010).

[2] McKhann G, Drachman D, Folstein M, Katzman R, Price D, Stadlan EM. Clinical diagnosis of Alzheimer's disease: report of the NINCDS–ADRDA Work Group under the auspices of Department of Health and Human Services Task Force on Alzheimer's Disease. Neurology 34: 939-944 (1984).

[3] Braak H, Braak E. Neuropathological stageing of Alzheimer-related changes. Acta Neuropathol 82: 239-259 (1991).

[4] Young J, Modat M, Cardoso MJ, Mendelson A, Cash D, Ourselin S. Accurate multimodal probabilistic prediction of conversion to Alzheimer's disease in patients with mild cognitive impairment. NeuroImage Clin 2: 735-745 (2013).

[5] Dubois B, Feldman HH, Jacova C, Cummings JL, Dekosky ST, Barberger-Gateau P. Revising the definition of Alzheimer's disease: a new lexicon. Lancet Neurol 9: 1118-1127 (2010).

[6] Modrego PJ. Predictors of conversion to dementia of probable Alzheimer type in patients with mild cognitive impairment. Curr Alzheimer Res 3: 161-170 (2006).

[7] Chupin M, Gérardin E, Cuingnet R, Boutet C, Lemieux L, Lehéricy S, *et al.* Fully automatic hippocampus segmentation and classification in Alzheimer's disease and mild cognitive impairment applied on data from ADNI. Hippocampus 19: 579-587 (2009).

[8] Duvernoy HM. The Human Hippocampus, Functional Anatomy, Vascularization and Serial Sections with MRI. Berlin: Springer (2005).

[9] Schonheit B, Zarski R, Ohm TG. Spatial and temporal relationships between plaques and tangles in Alzheimer-pathology. Neurobiol Aging 25(6): 697-711 (2004).

[10] Rössler M, Zarski R, Bohl J, Ohm TG. Stage-dependent and sector-specific neuronal loss in hippocampus during Alzheimer's disease. Acta Neuropathol 103: 363-369 (2002).

[11] Lace G, Savva GM, Forster G, de Silva R, Brayne C, Matthews FE, *et al.* Hippocampal tau pathology is related to neuroanatomical connections: an ageing population-based study. Brain 132: 1324-1334 (2009).

[12] Apostolova LG, Dutton RA, Dinov ID, Hayashi KM, Toga AW, Cummings JL, *et al.* Conversion of mild cognitive impairment to Alzheimer disease predicted by hippocampal atrophy maps. Arch Neurol 63(5): 693-699 (2006).

[13] Chételat G, Fouquet M, Kalpouzos G, Denghien I, De la Sayette V, Viader F, *et al.* Three-dimensional surface mapping of hippocampal atrophy progression from MCI to AD and over normal aging as assessed using voxel-based morphometry. Neuropsychologia 46(6): 1721-1731 (2008).

[14] La Joie R, Perrotin A, de La Sayette V, Egret S, Doeuvre L, Belliard S, *et al.* Hippocampal subfield volumetry in mild cognitive impairment, Alzheimer's disease and semantic dementia. NeuroImage Clin 3: 155-162 (2013).

[15] Pluta J, Yushkevich P, Das S, Wolk D. *In vivo* analysis of hippocampal subfield atrophy in mild cognitive impairment via semi-automatic segmentation of T2-weighted MRI. J Alzheimers Dis 31: 85-99 (2012).

[16] Frisoni GB, Ganzola R, Canu E, Rb U, Pizzini FB, Alessandrini F, *et al.* Mapping local hippocampal changes in alzheimer's disease and normal ageing with MRI at 3 tesla. Brain 131: 3266-3276 (2008).

[17] Mueller SG, Weiner MW. Selective effect of age Apo e4 and Alzheimer's disease on hippocampal subfields. Hippocampus 19: 558-564 (2009).

[18] Carmichael O, Mungas D, Beckett L, Harvey D, Tomaszewski Farias S, Reed B, *et al.* MRI predictors of cognitive change in a diverse and carefully characterized elderly population. Neurobiol Aging 33: 83-95 (2012).

[19] Hanseeuw BJ, Van Leemput K, Kavec M, Grandin C, Seron X, Ivanoiu A. Mild cognitive impairment: differential atrophy in the hippocampal subfields. AJNR: Am J Neuroradiol 32: 1658-1661 (2011).

[20] Larrieu S, Letenneur L, Orgogozo JM, Fabrigoule C, Amieva H, Le Carret N, *et al.* Incidence and outcome of mild cognitive impairment in a population-based prospective cohort. Neurology 59(10): 1594-1599 (2002).

[21] Van Leemput K, Bakkour A, Benner T, Wiggins G, Wald LL, Augustinack J. Automated segmentation of hippocampal subfields from ultra-high resolution *in vivo* MRI. Hippocampus 19: 549-557 (2009).

[22] Jack Jr CR, Bernstein MA, Fox NC, Thompson P, Alexander G, Harvey D, *et al.* The Alzheimer's Disease Neuroimaging Initiative (ADNI): MRI methods. J Magn Reson Imaging 27: 685-691 (2008).

[23] Dale AM, Fischl B, Sereno MI. Cortical surface-based analysis. I. Segmentation and surface reconstruction. Neuroimage 9: 179-194 (1999).

[24] Fischl B, Salat DH, Busa E, Albert M, Dieterich M, Haselgrove C, *et al.* Whole brain segmentation: automated labeling of neuroanatomical structures in the human brain. Neuron 33: 341-355 (2002).

[25] Ségonne F, Dale AM, Busa E, Glessner M, Salat D, Hahn HK, *et al.* A hybrid approach to the skull stripping problem in MRI. Neuroimage 22: 1060-1075 (2004).

[26] Fischl B, Salat DH, van der Kouwe AJ, Makris N, Ségonne F, Quinn BT, *et al.* Sequence-independent segmentation of magnetic resonance images. Neuroimage 23(1): S69-84 (2004).

[27] Chang CC and Lin CJ. LIBSVM: a library for support vector machines, 2001. Software available at http://www.csie.ntu.edu.tw/~cjlin/libsvm.

[28] Riedmiller M, Braun H. A direct adaptive method for faster backpropagation learning: The RPROP algorithm, Proceedings of the IEEE International Conference on Neural Networks. Pp. 586-591 (1993).

[29] Padurariu M, Ciobica A, Mavroudis I, Fotiou D, Baloyannis S. Hippocampal neuronal loss in the CA1 and CA3 areas of Alzheimer's disease patients. Psychiatr Danub 24(2): 152-158 (2012).

[30] Giannakopoulos P, Kovari E, Gold G, von Gunter A, Hof PR, Bowas C. Pathological substrates of cognitive decline in Alzheimer's disease. Front Neurol Neurosci 24: 20-29 (2009).

[31] West MJ, Kawas CH, Stewart WF, Rudow GL, Troncoso JC. Hippocampal neurons in pre-clinical Alzheimer's disease. Neurobiol Aging 25(9): 1205-12 (2004).

[32] Apostolova LG, Thompson PM, Green AE, Hwang KS, Zoumalan C, Jack CR, *et al.* 3D comparison of low, intermediate, and advanced hippocampal atrophy in MCI. Hum Brain Mapp 315: 786-797 (2010).

[33] Chételat G, Fouquet M, Kalpouzos G, Denghien I, De la Sayette V, Viader F, *et al.* Three-dimensional surface mapping of hippocampal atrophy progression from MCI to AD and over normal aging as assessed using voxel-based morphometry. Neuropsychologia 46(6): 1721-1731 (2008).

[34] Csernansky JG, Wang L, Swank J, Miller JP, Gado M, McKeel D, *et al.* Preclinical detection of Alzheimer's disease: hippocampal shape and volume predict dementia onset in the elderly. Neuroimage 25(3): 783-792 (2005).

[35] Wang L, Miller JP, Gado MH, McKeel DW, Rothermich M, Miller MI, *et al.* Abnormalities of hippocampal surface structure in very mild dementia of the Alzheimer type. Neuroimage 30(1): 52-60 (2006).

[36] Mueller SG, Schuff N, Yaffe K, Madison C, Miller B, Weiner MW. Hippocampal atrophy patterns in mild cognitive impairment

and Alzheimer's disease. Hum Brain Mapp 31(9): 1339-1347 (2010).

[37] de Flores R, La Joie R, Landeau B, Perrotin A, Mézenge F, de La Sayette V, *et al.* Effects of age and Alzheimer's disease on hippocampal subfields: Comparison between manual and freesurfer volumetry. Hum Brain Mapp 36(2): 463-74 (2015).

[38] Pipitone J, Park MT, Winterburn J, Lett TA, Lerch JP, Pruessner JC, *et al.* Multi-atlas segmentation of the whole hippocampus and subfields using multiple automatically generated templates. Neuroimage 101: 494-512 (2014).

[39] Frankó E, Olivier J, and Alzheimer's Disease Neuroimaging Initiative. Evaluating Alzheimer's disease progression using rate of regional hippocampal atrophy. PloS One 8(8) : e71354 (2013).

[40] Tang X, Holland D, Dale AM, Younes L, Miller MI. Shape abnormalities of subcortical and ventricular structures in mild cognitive impairment and Alzheimer's disease: detecting, quantifying, and predicting. Hum Brain Mapp 35(8): 3701-3725 (2014).

[41] Wisse LE, Gerritsen L, Zwanenburg JJ, Kuijf HJ, Luijten PR, Biessels GJ, *et al.* Subfields of the hippocampal formation at 7 T MRI: *in vivo* volumetric assessment. Neuroimage 61(4): (2012).

[42] Wisse, LE, Biessels G, Geerlings MI. A critical appraisal of the hippocampal subfield segmentation package in FreeSurfer. Front Aging Neurosci 6 : 261 (2014).

[43] Schuff N. A new sensitive MRI marker for memory deficits in normal aging. Neurology 74(3): 188-189 (2010).

[44] Carlesimo GA, Cherubini A, Caltagirone C, Spalletta G. Hippocampal mean diffusivity and memory in healthy elderly individuals: a cross-sectional study. Neurology 74(3): 194-200 (2010).

Received: April 20, 2015 **Revised: October 16, 2015** **Accepted: November 12, 2015**